ChemComm

COMMUNICATION

View Article Online
View Journal | View Issue

Cite this: *Chem. Commun.*, 2020, **56**, 7309

Received 29th April 2020,
Accepted 21st May 2020

DOI: 10.1039/d0cc03091k

rsc.li/chemcomm

Biomimetic asymmetric reduction of benzoxazinones and quinoxalinones using ureas as transfer catalysts†

Zi-Biao Zhao, [ab] Xiang Li,[a] Mu-Wang Chen, [c] Zongbao K. Zhao [*c] and Yong-Gui Zhou [*abc]

Using ureas as transfer catalysts through hydrogen bonding activation, biomimetic asymmetric reduction of benzoxazinones and quinoxalinones with chiral and regenerable NAD(P)H models was described, giving chiral dihydrobenzoxazinones and dihydroquinoxalinones with high yields and excellent enantioselectivities. A key dihydroquinoxalinone intermediate of a BRD4 inhibitor was synthesized using biomimetic asymmetric reduction.

The development of biomimetic science has brought great benefits to human life. The reduced nicotinamide adenine dinucleotide (NADH) and nicotinamide adenine dinucleotide phosphate (NADPH) as crucial redox coenzymes play a vital role in cells. The interconversion of the pyridine nucleotide coenzymes NAD(P)+/NAD(P)H is widespread in over 400 enzymatic reactions (Scheme 1a).[1] Because these coenzymes are expensive and labile, synthetic NAD(P)H mimics have continuously emerged over the past decades. Early works mainly focused on the development of the stoichiometric NAD(P)H models such as dihydronicotinamide derivatives,[2] Hantzsch esters (HEH),[3] benzothiazolines,[4] *etc.* The utilization of the stoichiometric models limits its further regeneration and leads to low atomic economy. Subsequently, regenerable NAD(P)H models were devised and the processes were realized by *in situ* regeneration mediated by homogeneous catalysts including rhodium,[5] ruthenium,[6] iron,[7] sodium dithionate,[8] *etc.*[9] In terms of biomimetic asymmetric reduction, stereocontrol is mainly provided by the chiral transfer catalysts.[6,7b] Nevertheless, chiral transfer catalyst screening is quite tedious in each biomimetic reduction. Very recently, a chiral and regenerable NAD(P)H model based on a ferrocene-derived motif was designed and employed for biomimetic asymmetric reduction[10] (Scheme 1b). The readily available and bench-stable achiral Lewis acids[10] and Brønsted acids[11] could be used as transfer catalysts. These two types of transfer catalysts have different activation modes.[11] However, these catalysts have limited compatibility with acid-labile or polyfunctional substrates and tandem transformations.[12] Therefore, more mild and general transfer catalysts remain to be developed, especially those with potentially new activation modes, to further expand the generality of biomimetic asymmetric reduction.

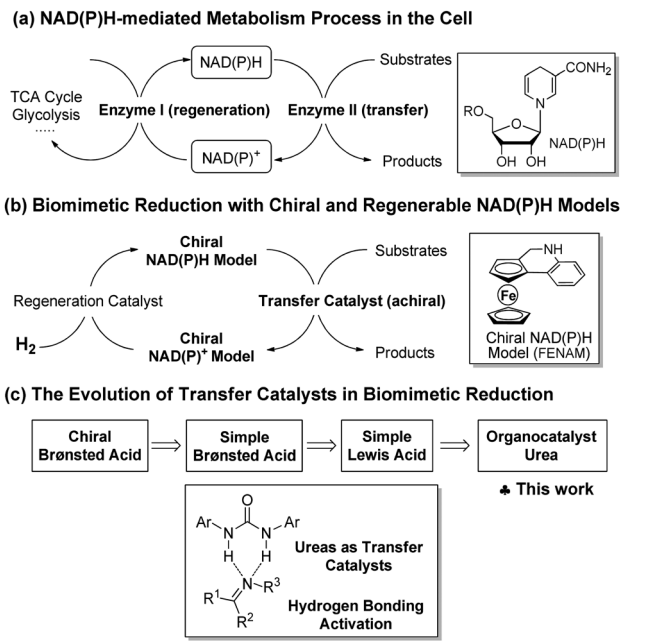

Scheme 1 Biomimetic asymmetric reduction (BMAR) based on the coenzyme NAD(P)H and transfer catalysts.

[a] *Zhang Dayu School of Chemistry, Dalian University of Technology, Dalian 116024, P. R. China*
[b] *State Key Laboratory of Organometallic Chemistry, Shanghai Institute of Organic Chemistry, Chinese Academy of Sciences, Shanghai 200032, P. R. China*
[c] *State Key Laboratory of Catalysis, Dalian Institute of Chemical Physics, Chinese Academy of Sciences, Dalian 116023, P. R. China.*
E-mail: zhaozb@dicp.ac.cn, ygzhou@dicp.ac.cn

† Electronic supplementary information (ESI) available. See DOI: 10.1039/d0cc03091k

Hydrogen-bonding interaction plays an important role in the molecular recognition and activation processes of various biologically important reactions. (Thio)urea-based bifunctional catalysts capable of activating substrates through hydrogen-bonding activity have received much attention.[13] (Thio)urea derivatives feature good functional group tolerance, and they are cheap, moisture-insensitive, and readily accessible. Therefore, catalysis through hydrogen-bonding interaction has been introduced as a powerful methodology for asymmetric reaction.[13] However, no report on the application of this method to biomimetic reduction with chiral NAD(P)H models has appeared. Hence, the development of a novel activation method in biomimetic reduction with chiral and regenerable NAD(P)H models is significant in organic chemistry. In this paper, we present biomimetic asymmetric reduction through a hydrogen-bonding activation strategy using urea derivatives (Scheme 1c).

To validate our proposed activation strategy, we chose benzoxazinone (**1a**) as the model substrate with the chiral and regenerable NAD(P)H model (*R*)-**H1** and (thio)urea derivatives as transfer catalysts. The results of condition optimization are summarized in Table 1. The present study was initiated by direct biomimetic reduction in the absence of transfer catalysts, unfortunately, only <5% of the desired product was observed (entry 1). To our delight, the reaction could be carried out smoothly using the urea derivatives. The desired product was obtained in 92% enantioselectivity albeit with a low 10% yield (entry 2). Next, a number of solvents were extensively examined. It was found that $CHCl_3$ was the best choice in terms of yields and enantioselectivity (entries 2–7). Subsequently, considering the effect of temperature on the reaction, we tried to increase the temperature. When the reaction was carried out at 70 °C, the reaction gave the desired product with 82% yield and 96% ee value (entry 9). However, when the reaction temperature is further increased, the NAD(P)H model based on the ferrocene-derived structure is inactivated (entry 10). Subsequently, we turned our attention to a series of organic hydrogen-bonding catalysts. When replacing urea with thiourea, the reaction did not occur (entry 11), which might be ascribed to the strong poisonous effect of thiourea on the ruthenium regeneration catalyst. We found that the urea and squaramide catalysts could make the reaction proceed smoothly and urea OC-**3** proved to be the best (entries 9, 12–14). Besides, it was noted that the desirable hydrogenation product could be obtained albeit with low conversion using the mono hydrogen bonding donor OC-**6** (58% conversion, 94% ee) and the fully *N*-methyl protected urea OC-**7** (11% conversion, 87% ee) as transfer catalyst (entries 15 and 16).

Hereafter, further examinations focused on screening of chiral and regenerable NAD(P)H models (Table 2). NAD(P)H models with planar chirality were favourable and the best result was achieved with (*R*)-**H1**. It is worth noting that the electronic properties of the substituents on the structure have obvious effects on the results (entries 2 and 3). In addition, other NAD(P)H models with axial chirality including the nitrogen atom close to the C2 axial stereocenter and the nitrogen atom

Table 1 Optimization of reaction parameters[a]

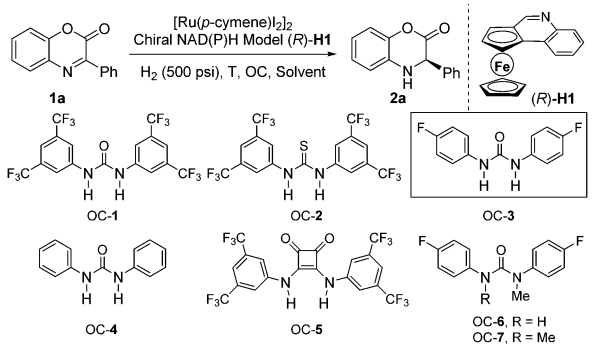

Entry	OC	Solvent	T (°C)	Convn.[b] (%)	Ee[c] (%)
1	—	Toluene	50	<5	—
2	OC-**1**	Toluene	50	10	92
3	OC-**1**	Benzene	50	12	95
4	OC-**1**	DCM	50	28	93
5	OC-**1**	$CHCl_3$	50	24	96
6	OC-**1**	DCE	50	35	91
7	OC-**1**	THF	50	<5	—
8	OC-**1**	$CHCl_3$	60	30	96
9	OC-**1**	$CHCl_3$	70	82	96
10	OC-**1**	$CHCl_3$	80	60	92
11	OC-**2**	$CHCl_3$	70	<5	—
12	OC-**3**	$CHCl_3$	70	85	96
13	OC-**4**	$CHCl_3$	70	30	94
14	OC-**5**	$CHCl_3$	70	33	97
15	OC-**6**	$CHCl_3$	70	58	94
16	OC-7	$CHCl_3$	70	11	87

[a] Reaction conditions: **1a** (0.10 mmol), $[Ru(p\text{-cymene})I_2]_2$ (0.5 mol%), (*R*)-**H1** (10 mol%), OC (20 mol%), solvent (2 mL), H_2 (500 psi), 50 °C, and 24 h. [b] Conversion was measured by analysis of ^{1}H NMR spectra. [c] Determined by HPLC.

Table 2 Optimization of chiral NAD(P)H models[a]

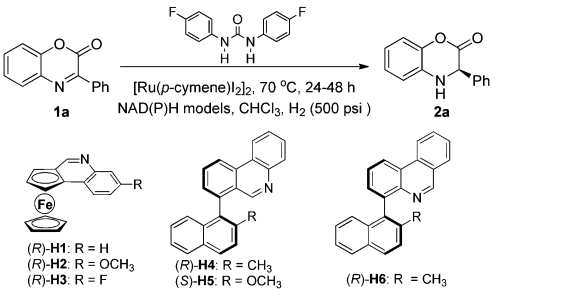

Entry	Chiral NAD(P)H model	Convn.[b] (%)	Ee[c] (%)
1	(*R*)-**H1**	85	96
2	(*R*)-**H2**	45	94
3	(*R*)-**H3**	18	83
4	(*R*)-**H4**	9	14
5	(*S*)-**H5**	29	53
6	(*R*)-**H6**	<5	—
7[d]	(*R*)-**H1**	94	95

[a] Reaction conditions: **1a** (0.10 mmol), $[Ru(p\text{-cymene})I_2]_2$ (0.5 mol%), chiral NAD(P)H model (10 mol%), OC-**3** (20 mol%), $CHCl_3$ (2 mL), H_2 (500 psi), 70 °C, and 24 h. [b] Conversion was measured by analysis of ^{1}H NMR spectra. [c] Determined by HPLC. [d] 48 h.

far away from the C2 axial stereocenter have also been investigated. Unfortunately, these NAD(P)H models only deliver trace amounts of product (entries 4–6). In order to enhance the conversion, the reaction time was increased to 48 h with improved activity and almost the same ee. Therefore, the optimal conditions were established.

With the optimized conditions in hand, the reaction scope of benzoxazinones was then evaluated, and the results are summarized in Scheme 2. These results revealed that this strategy was suitable for a series of benzoxazinones. The electronic and steric effects on the phenyl of the substrate slightly influenced the reactivity and enantioselectivity (**2a**–**2g**). For example, the ee value was reduced to 88% when the electron-donating methoxy group was at the *para*-position of the aryl moiety (**2c**). Gratifyingly, the desired product could be obtained with high reactivity and enantioselectivity when the methoxy group was at the *ortho*-position of the aryl moiety (**2g**). Subsequently, we investigated disubstituents at the phenyl and different groups at the benzoxazinone skeleton (**2h**–**2j**). Moreover, the alkyl-substituted substrates were also amenable to the present reaction, delivering the products in high yields and excellent enantioselectivity (**2k**–**2l**).

To expand the generality of this strategy, we next focused on the biomimetic asymmetric reduction of quinoxalinones with the NAD(P)H model and the urea catalyst. The results are depicted in Scheme 3. In the case of the aromatic moiety, the reaction conditions tolerated both electron-donating and electron-withdrawing substituents (**4a**–**4g**). It was found that the enantioselectivity was slightly reduced when the methyl was at the *para*-position (**4d**). Meanwhile, when the methoxy group is at the *para*-position and *ortho*-position (**4e**–**4f**), the enantioselectivity was slightly lower than with methyl. Notably, when the fluorine group was introduced to the *meta*-position of the aryl structure, the reaction proceeded smoothly, giving the desired product with excellent enantioselectivity and yield (**4g**). Furthermore, the allyl-substituted substrate was also well compatible to deliver the corresponding product with 95% yield and 93% enantioselectivity (**4h**). It is worth noting that the alkyl-substituted substrate was also investigated, and a 97% yield and 90% enantioselectivity could be obtained under the optimal conditions (**4i**).

As a member of the family of the bromodomain and extra-terminal domain (BET) proteins, bromodomain-containing protein 4 (BRD4) is a feasible drug target for cancer treatment on the basis of recent biological and pharmacological studies.[14] A series of novel dihydroquinoxalinone derivatives could be used as BRD4 inhibitors. Therefore, we performed a concise synthesis of a key intermediate of a BRD4 inhibitor using the above methodology (Scheme 4). Under the standard conditions, bromine-substituted quinoxalinone **3j** afforded the desired

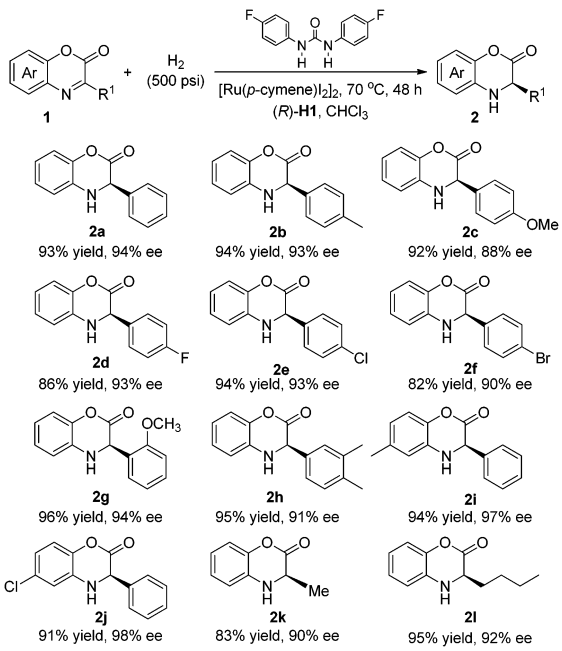

Scheme 2 The BMAR of benzoxazinones. Reaction conditions: **1** (0.20 mmol), $[Ru(p\text{-cymene})I_2]_2$ (0.5 mol%), (*R*)-**H1** (10 mol%), OC-**3** (20 mol%), $CHCl_3$ (3 mL), H_2 (500 psi), 70 °C, and 48 h.

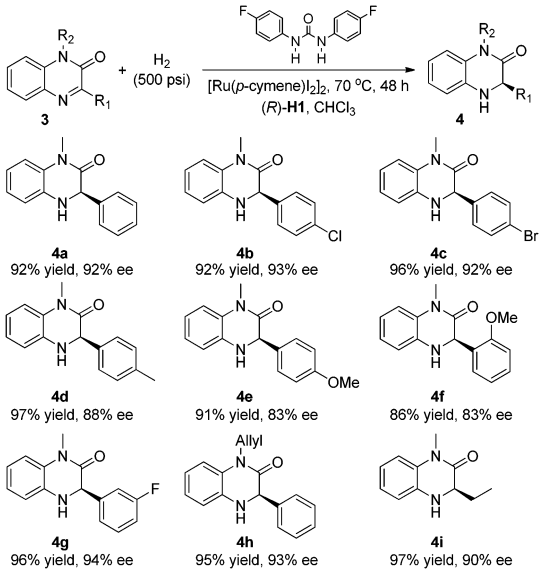

Scheme 3 The BMAR of quinoxalinones. Reaction conditions: **3** (0.20 mmol), $[Ru(p\text{-cymene})I_2]_2$ (0.5 mol%), (*R*)-**H1** (10 mol%), OC-**3** (20 mol%), $CHCl_3$ (3 mL), H_2 (500 psi), 70 °C, and 48 h.

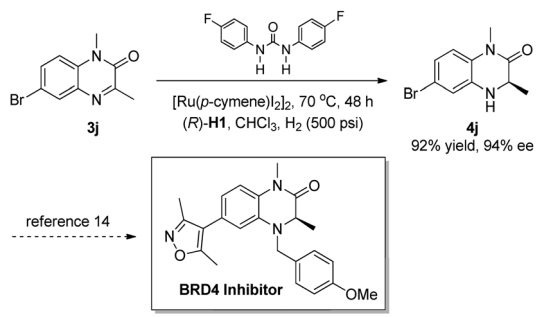

Scheme 4 The BMAR of bromine-substituted quinoxalinone and synthesis of a key intermediate of a BRD4 inhibitor.

product with 92% yield and 94% ee, which is a key intermediate for the synthesis of a BRD4 inhibitor.[14a]

Based on the experimental results, a plausible mechanism and transition state model are illustrated in Fig. S1 (see ESI†). The urea catalysts promote the reduction through hydrogen-bonding activation. The chiral NAD(P)H model transfers the hydrogen atom from the less steric face to the imine, leading to the (*R*)-products.

In summary, we have disclosed a hydrogen-bonding activation strategy for biomimetic asymmetric reduction with chiral and regenerable NAD(P)H models. This methodology could be extended to benzoxazinone and quinoxalinone substrates for furnishing chiral products with high yields and excellent enantioselectivity. A key dihydroquinoxalinone intermediate of a BRD4 inhibitor was synthesized using the biomimetic asymmetric reduction methodology. This activation method will further broaden the generality of biomimetic asymmetric reduction. Further, investigation of other activation modes and substrate scope is under progress and the results will be presented in due course.

We are grateful for the financial support from the National Natural Science Foundation of China (21532006) and the Chinese Academy of Sciences (XDB17020300 and QYZDJ-SSW-SLH035).

Conflicts of interest

There are no conflicts to declare.

Notes and references

1 For reviews see: (*a*) J. Gebicki, A. Marcinek and J. Zielonka, *Acc. Chem. Res.*, 2004, **37**, 379; (*b*) R. H. Houtkooper, C. Cantó, R. J. Wanders and J. Auwerx, *Endocr. Rev.*, 2010, **31**, 194; (*c*) H. Wu, C. Tian, X. Song, C. Liu, D. Yang and Z. Jiang, *Green Chem.*, 2013, **15**, 1773.

2 For reviews see: (*a*) N.-X. Wang and J. Zhao, *Synlett*, 2007, 2785; (*b*) C.-B. Bai, N.-X. Wang, Y. Xing and X.-W. Lan, *Synlett*, 2017, 402. For selected examples, see: (*c*) Y. Ohnishi, M. Kagami and A. Ohno, *J. Am. Chem. Soc.*, 1975, **97**, 4766; (*d*) N. Kanomata and T. Nakata, *J. Am. Chem. Soc.*, 2000, **122**, 4563.

3 For reviews see: (*a*) S.-L. You, *Chem. – Asian J.*, 2007, **2**, 820; (*b*) S. G. Ouellet, A. M. Walji and D. W. C. Macmillan, *Acc. Chem. Res.*, 2007, **40**, 1327; (*c*) S. J. Connon, *Org. Biomol. Chem.*, 2007, **5**, 3407; (*d*) C. Wang, X. Wu and J. Xiao, *Chem. – Asian J.*, 2008, **3**, 1750; (*e*) M. Rueping, J. Dufour and F. R. Schoepke, *Green Chem.*, 2011, **13**, 1084; (*f*) C. Zheng and S.-L. You, *Chem. Soc. Rev.*, 2012, **41**, 2498; (*g*) A. M. F. Phillips and A. J. L. Pombeiro, *Org. Biomol. Chem.*, 2017, **15**, 2307. For selected examples, see: (*h*) M. Rueping, E. Sugiono, C. Azap, T. Theissmann and M. Bolte, *Org. Lett.*, 2005, **7**, 3781; (*i*) J. W. Yang, M. T. Hechavarria Fonseca, N. Vignola and B. List, *Angew. Chem., Int. Ed.*, 2005, **44**, 108; (*j*) S. G. Ouellet, J. B. Tuttle and D. W. C. MacMillan, *J. Am. Chem. Soc.*, 2005, **127**, 32; (*k*) S. Mayer and B. List, *Angew. Chem., Int. Ed.*, 2006, **45**, 4193; (*l*) N. J. A. Martin and B. List, *J. Am. Chem. Soc.*, 2006, **128**, 13368; (*m*) J. W. Yang and B. List, *Org. Lett.*, 2006, **8**, 5653; (*n*) Z. Wang, F. Ai, Z. Wang, W. Zhao, G. Zhu, Z. Lin and J. Sun, *J. Am. Chem. Soc.*, 2015, **137**, 383.

4 For recent review see: (*a*) C. Zhu, K. Saito, M. Yamanaka and T. Akiyama, *Acc. Chem. Res.*, 2015, **48**, 388. For selected examples, see: (*b*) C. Zhu and T. Akiyama, *Org. Lett.*, 2009, **11**, 4180; (*c*) C. Zhu and T. Akiyama, *Synlett*, 2011, 1251; (*d*) J.-Q. Zhou, W.-J. Sheng, J.-H. Jia, Q. Ye, J.-R. Gao and Y.-X. Jia, *Tetrahedron Lett.*, 2013, **54**, 3082; (*e*) K. Saito, K. Horiguchi, Y. Shibata, M. Yamanaka and T. Akiyama, *Chem. – Eur. J.*, 2014, **20**, 7616; (*f*) K. Horiguchi, E. Yamamoto, K. Saito, M. Yamanaka and T. Akiyama, *Chem. – Eur. J.*, 2016, **22**, 8078.

5 H. C. Lo and R. H. Fish, *Angew. Chem., Int. Ed.*, 2002, **41**, 478.

6 For selected examples, see: (*a*) Q.-A. Chen, M.-W. Chen, C.-B. Yu, L. Shi, D.-S. Wang, Y. Yang and Y.-G. Zhou, *J. Am. Chem. Soc.*, 2011, **133**, 16432; (*b*) Q.-A. Chen, K. Gao, Y. Duan, Z.-S. Ye, L. Shi, Y. Yang and Y.-G. Zhou, *J. Am. Chem. Soc.*, 2012, **134**, 2442; (*c*) M.-W. Chen, B. Wu, Z.-P. Chen, L. Shi and Y.-G. Zhou, *Org. Lett.*, 2016, **18**, 4650; (*d*) Z.-P. Chen, M.-W. Chen, R.-N. Guo and Y.-G. Zhou, *Org. Lett.*, 2014, **16**, 1406.

7 For selected examples, see: (*a*) L.-Q. Lu, Y. Li, K. Junge and M. Beller, *Angew. Chem., Int. Ed.*, 2013, **52**, 8382; (*b*) L.-Q. Lu, Y. Li, K. Junge and M. Beller, *J. Am. Chem. Soc.*, 2015, **137**, 2763.

8 B. Procuranti and S. J. A. Connon, *Chem. Commun.*, 2007, 1421.

9 L. Zhao, J. Wei, J. Lu, C. He and C. Duan, *Angew. Chem., Int. Ed.*, 2017, **56**, 8692.

10 J. Wang, Z.-H. Zhu, M.-W. Chen, Q.-A. Chen and Y.-G. Zhou, *Angew. Chem., Int. Ed.*, 2019, **58**, 1813.

11 (*a*) J. Wang, Z.-B. Zhao, Y. Zhao, G. Luo, Z.-H. Zhu, Y. Luo and Y.-G. Zhou, *J. Org. Chem.*, 2020, **85**, 2355; (*b*) Z.-B. Zhao, X. Li, B. Wu and Y.-G. Zhou, *Chin. J. Chem.*, 2020, **38**, 714.

12 For some selected examples, see: (*a*) R. Kadyrov and T. H. Riermeier, *Angew. Chem., Int. Ed.*, 2003, **42**, 5472; (*b*) D. Menche, J. Hassfeld, J. Li, G. Menche, A. Ritter and S. Rudolph, *Org. Lett.*, 2006, **8**, 741.

13 For reviews see: (*a*) P. R. Schreiner, *Chem. Soc. Rev.*, 2003, **32**, 289; (*b*) J. Seayad and B. List, *Org. Biomol. Chem.*, 2005, **3**, 719; (*c*) Y. Takemoto, *Org. Biomol. Chem.*, 2005, **3**, 4299; (*d*) S. J. Connon, *Chem. – Eur. J.*, 2006, **12**, 5418; (*e*) M. S. Taylor and E. N. Jacobsen, *Angew. Chem., Int. Ed.*, 2006, **45**, 1520; (*f*) A. G. Doyle and E. N. Jacobsen, *Chem. Rev.*, 2007, **107**, 5713; (*g*) C. Grondal, M. Jeanty and D. Enders, *Nat. Chem.*, 2010, **2**, 167; (*h*) X. Fang and C.-J. Wang, *Chem. Commun.*, 2015, **51**, 1185. For selected examples, see: (*i*) D. P. Curran and L. H. Kuo, *J. Org. Chem.*, 1994, **59**, 3259; (*j*) M. S. Sigman and E. N. Jacobsen, *J. Am. Chem. Soc.*, 1998, **120**, 4901; (*k*) A. Wittkopp and P. R. Schreiner, *Chem. – Eur. J.*, 2003, **9**, 407; (*l*) T. Okino, Y. Hoashi and Y. Takemoto, *J. Am. Chem. Soc.*, 2003, **125**, 12672; (*m*) M. S. Taylor and E. N. Jacobsen, *J. Am. Chem. Soc.*, 2004, **126**, 10558; (*n*) P. M. Pihko, *Angew. Chem., Int. Ed.*, 2004, **43**, 2062; (*o*) D. E. Fuerst and E. N. Jacobsen, *J. Am. Chem. Soc.*, 2005, **127**, 8964.

14 (*a*) Y. Yang, L. Zhao, B. Xu, L. Yang, J. Zhang, H. Zhang and J. Zhou, *Bioorg. Chem.*, 2016, **68**, 236; (*b*) M. Jung, K. A. Gelato, A. Fernández-Montalván, S. Siegel and B. Haendler, *Epigenomics*, 2015, **7**, 487.

